

**HOPE CREEK GENERATING STATION
FACILITY OPERATING LICENSE NPF-57
DOCKET NO. 50-354**

**REQUEST FOR LICENSE AMENDMENT
EXTENDED POWER UPRATE**

**Stress Analysis of the Hope Creek Unit 1 Steam Dryer for CLTP
CDI Report No. 05-25, Revision 0
November 2005**

Stress Analysis of the Hope Creek Unit 1 Steam Dryer for CLTP

Revision 0

Prepared by

Continuum Dynamics, Inc.
34 Lexington Avenue
Ewing, NJ 08618

Prepared under Purchase Order No. 4500283344 for

Nuclear Business Unit, PSEG Nuclear LLC
Materials Center, Alloway Creek Neck Road
Hancocks Bridge, NJ 08038

Approved by


Alan J. Bilanin

November 2005

Executive Summary

In this analysis, stresses induced by the flow of steam through the steam dryer at Hope Creek Unit 1 are calculated and evaluated at Current Licensed Thermal Power. The fluctuating pressure loads induced by the flowing steam were predicted by a separate acoustic circuit analysis of the steam dome and main steam lines, and these loads have been applied to the steam dryer structure.

Stresses resulting from the fluctuating steam flow load have been calculated using a finite element model (the ANSYS computer code). Loads were applied to the structure at 0.001 sec intervals for 0.5 sec (500 time steps), and the equations representing the structural dynamics were solved using a time history dynamic analysis. Special attention was paid to areas of high stress, including high weld stress.

The stress results have been evaluated for compliance with the ASME B&PV Code, Section III, subsection NG. The load combination for normal operation (the Level A Service Condition) has been evaluated. This combination consists almost entirely of the fluctuating pressure loads and weight. Evaluation is done for maximum stress, as well as for cyclic (fatigue type) stress. Level B service conditions, which include seismic, are not included in this evaluation.

The results for the Level A service condition show all stresses are low when compared to the allowable values, with a minimum stress ratio of 3.7 (stress ratio is the allowable stress divided by the calculated stress). Stress ratios for specific locations on the steam dryer are tabulated in Section VI.

This analysis includes all Hope Creek Unit 1 dryer modifications and accounts for current power generation rate. In case of further dryer modifications and/or power uprate, the analysis should be performed with an updated pressure load time history, calculated using acoustic circuit analysis and based on strain gage measurements in the main steam lines.

Table of Contents

Section	Page
Executive Summary	i
Table of Contents	ii
I. Introduction and Purpose.....	1
II. Model Description.....	2
2.1 Steam Dryer Geometry	2
2.2 Material Properties.....	5
2.3 Loading	5
III. Finite Element Model	7
3.1 Model Simplifications	7
3.2 Perforated Plate Model	7
3.3 Vane Bank Model	7
3.4 Water Inertia Effects on Submerged Panels	7
3.5 Structural Damping.....	8
3.6 Mesh Details and Element Types.....	8
IV. Dynamic Analysis.....	15
V. Results.....	16
5.1 General Stress Distribution	16
5.2 Maximum Stress Locations.....	17
VI. Load Combinations and Allowable Stress Intensities	24
6.1 Load Combinations for Evaluation	24
6.2 Allowable Stress Intensities.....	24
6.3 Comparison of Calculation and Alternating Stress Intensities	25
VII. Conclusions.....	26
VIII. References	27

I. Introduction and Purpose

Recent inspections of the steam dryers in Mark I plants have shown cracks in the fillet welds and nearby structure. The industry has addressed this problem with physical modifications to the dryers, as well as a program to define steam dryer loads and their resulting stresses.

Hope Creek Unit 1 (HC1) is part of this program. The plant has inspected its dryer, found some weld cracking, and has made structural modifications to correct this problem. The purpose of the stress analysis discussed here is to calculate stresses from the anticipated steam dryer loads at HC1 and compare those stresses to acceptance criteria from the ASME Code. This step will ensure that the modifications are adequate and that future weld cracking will not occur.

The damaging steam dryer loads are due to pressure fluctuations, induced by steam flow through the dryer. Over a long period of time, cyclic stresses from these loads can produce fatigue cracking if loads are sufficiently high. Since fillet welds are the most susceptible to fatigue failure, most of the failures have been found in these areas.

The fluctuating pressure loads, induced by the flowing steam, were predicted by a separate acoustic circuit analysis of the steam dome and main steam lines [1]. These loads are applied to the steam dryer structure in the following analysis.

Stresses resulting from the fluctuating steam flow load have been calculated using a finite element model (the ANSYS computer code). Loads were applied to the structure at 0.001 sec intervals for 0.5 sec (500 time steps), and the equations representing the structural dynamics were solved using a time history dynamic analysis. Special attention was paid to areas of high stress, including high weld stress.

The stress results are evaluated for compliance with the ASME B&PV Code, Section III, subsection NG. The load combination for normal operation (the Level A Service Condition) has been evaluated. This combination consists almost entirely of the fluctuating pressure loads and weight. Evaluation is done for maximum stress, as well as for cyclic (fatigue type) stress. Level B service conditions, which include seismic, are not included in this evaluation.

Results of the analysis are shown in Sections V and VI. They show that stresses for the modified structure are low and meet all ASME Code requirements with large margins of safety.

II. Model Description

A description of the ANSYS model of the HC1 steam dryer follows.

2.1 Steam Dryer Geometry

A geometry model of the HC1 steam dryer was developed from available drawings, as well as from field measurements taken by C.D.I. on a spare dryer. The completed model is shown in Figure 2.1.

This model includes modifications made to the HC1 steam dryer on-site, prior to commercial operations. These are:

- Tie bars, hoods, and end plates were replaced on the original dryer (FDI-041-79450)
- Reinforcement bars were added to the hoods (FDDR-KT1-415 and KT1-0444)

The modified areas are shown in Figure 2.2.

The level of steam dryer detail was chosen based on preliminary calculations using the ANSYS finite element model. Weld details were added in places where higher stresses were computed, namely, at drain pipe / trough bottom plate junctions and hood support / perforated plate junctions (Figure 2.3).

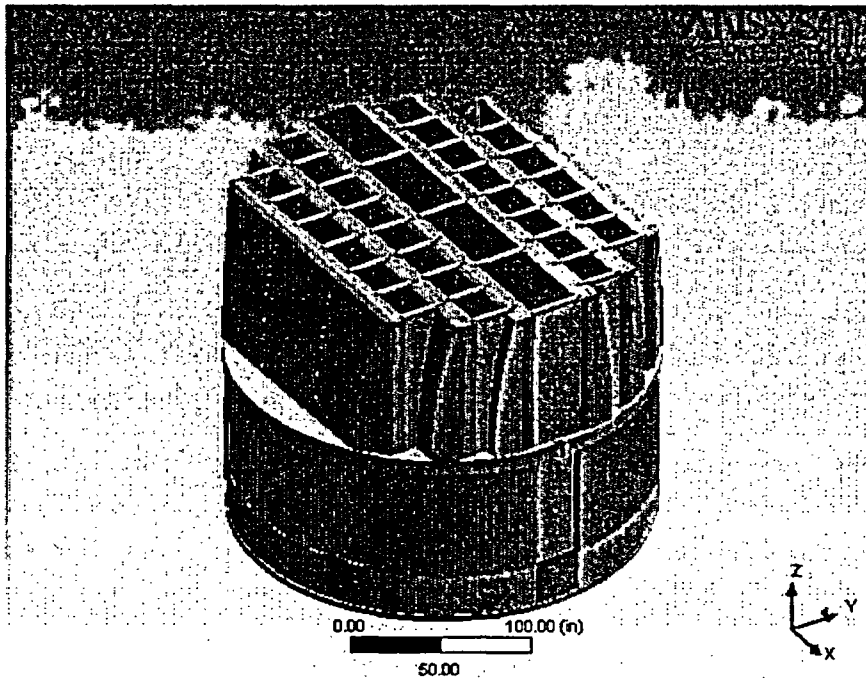


Figure 2.1. The geometry model of the HC1 steam dryer.

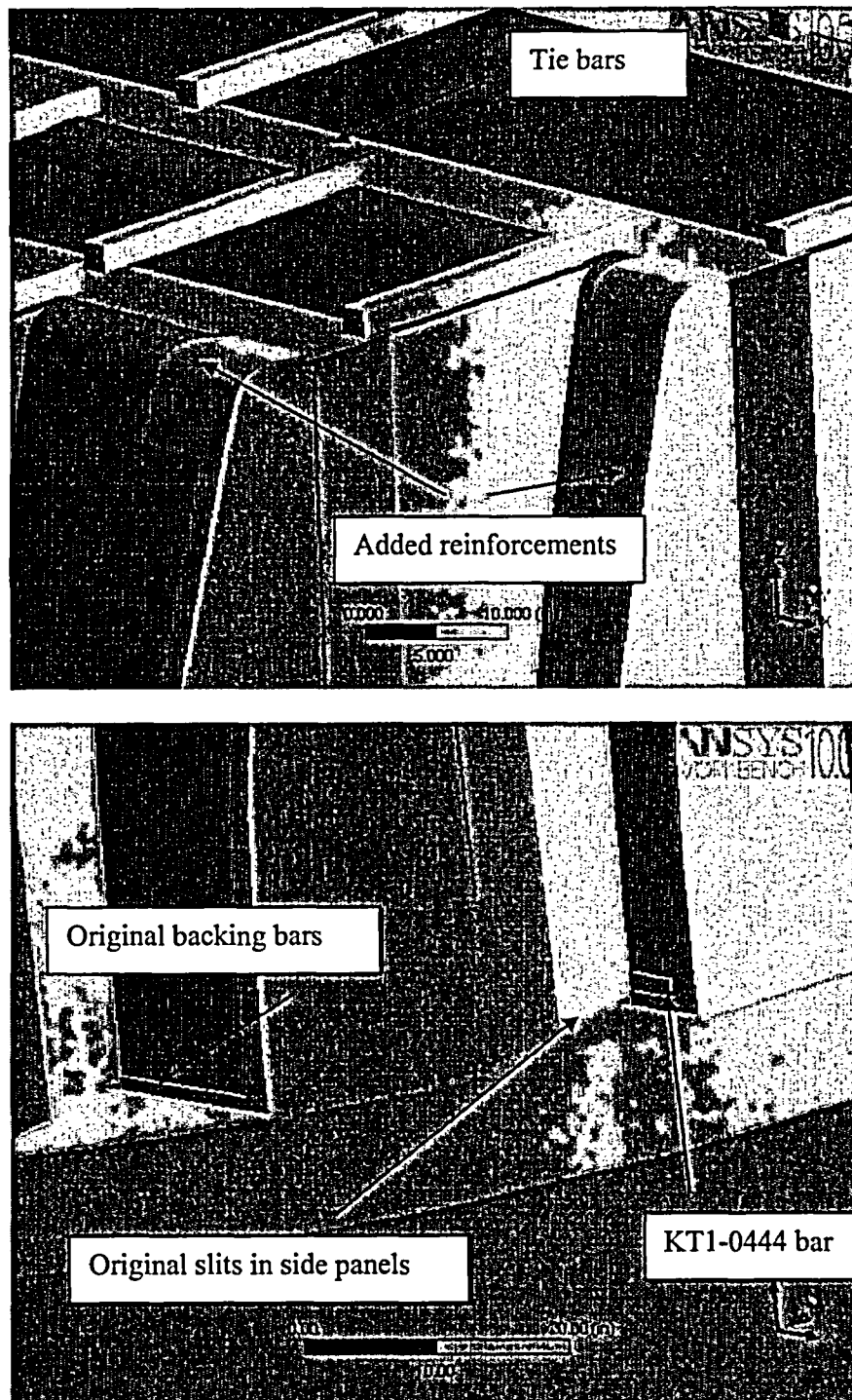


Figure 2.2. On-site modifications accounted for in the model and some details in geometry.

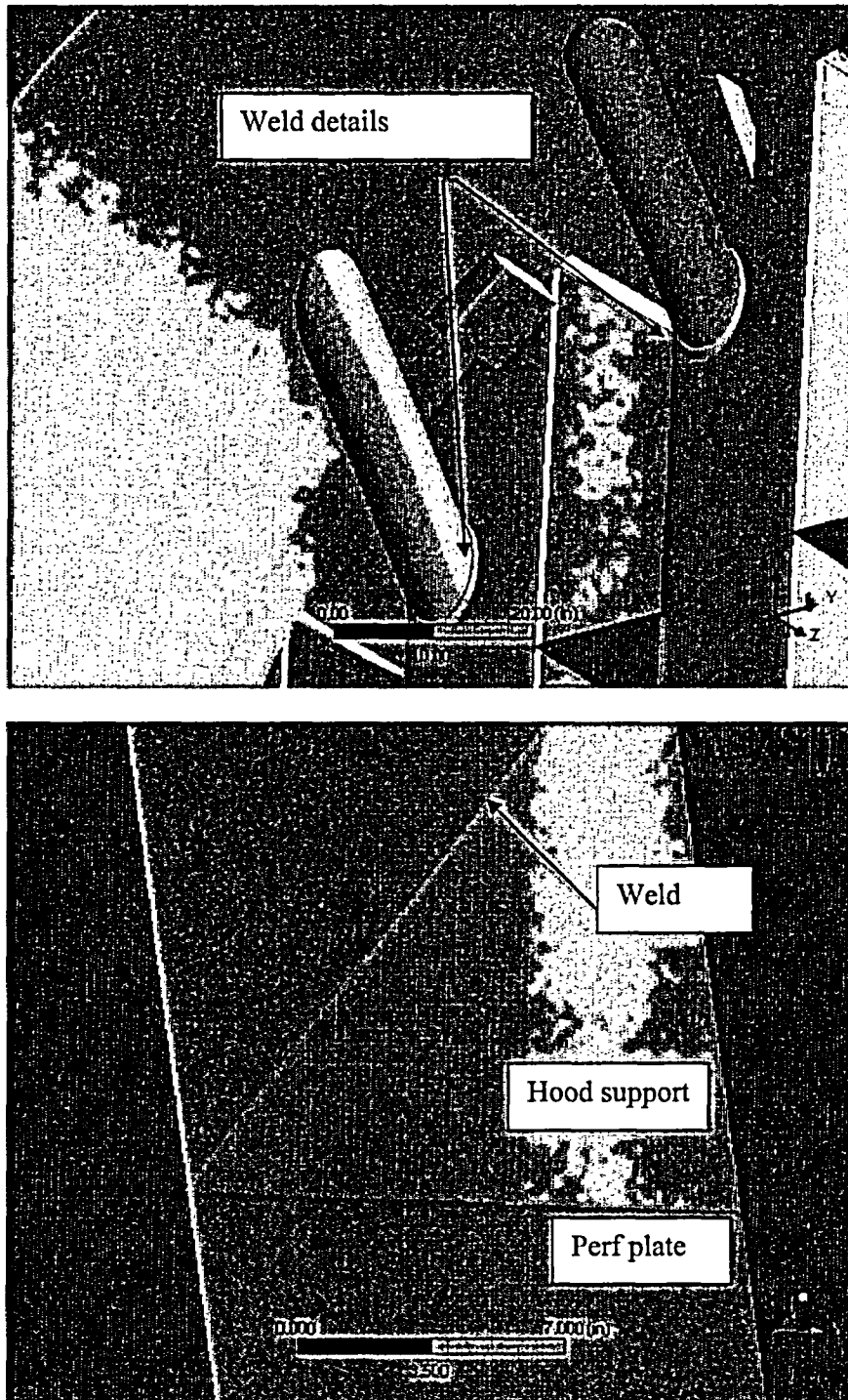


Figure 2.3. Weld details. Solid elements were added at all drain pipe / trough bottom plate junctions and all hood support / perforated plate junctions (both sides), at 28 locations on the dryer.

2.2 Material Properties

The steam dryer is constructed from Type 304 stainless steel and has an operating temperature of 550°F. Properties used in the analysis are summarized in Table 2.1.

Table 2.1. Material properties.

	Young's Modulus (10 ⁶ psi)	Density (lbm/in ³)	Poisson Ratio
Structural Steel	25.55	0.284	0.3
Structural Steel for Perforated Plates	15.33	0.227	0.3
Structural Steel with Added Water Inertia Effect	25.55	4.65	0.3

The structural steel modulus is from Appendix A of the ASME Code for Type 304 Stainless Steel at an operating temperature 550°F. Effective properties of perforated plates and submerged parts are discussed in Section III.

2.3 Loading

The pressure time history loading was obtained from an acoustic circuit model of the HC1 steam dryer, performed by C.D.I. and detailed in [1]. This loading was provided over the steam dryer surface on a three-inch grid, at a total of 10,963 locations. The time interval spanned the 0.5 sec of data that contained the peak minimum and maximum pressures on a low-resolution grid of the dryer (including only corners and edges, a total of 104 locations). The peak time history on the low-resolution grid is shown in Figure 2.4, at a location on the outer bank hood opposite the A and B main steam lines.

These results were interpolated onto the detailed structural grid of the HC1 steam dryer, and the ANSYS calculation was then undertaken. In addition to the fluctuating pressure load, all computer analysis included the weight of the steam dryer. The fluctuating pressure loads were applied to all surfaces, as indicated in Figure 2.5.

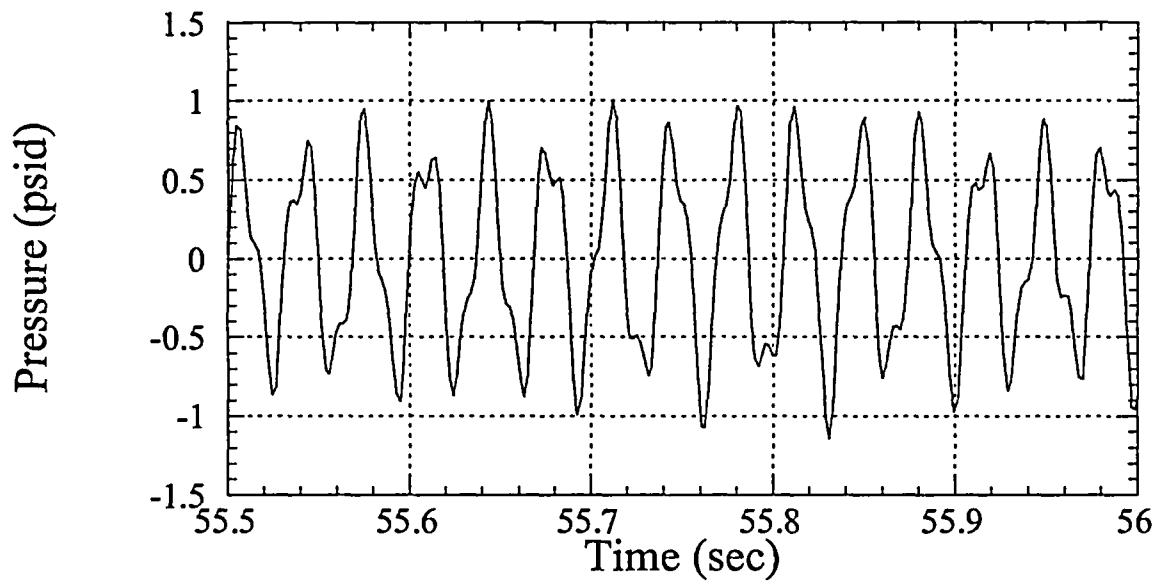


Figure 2.4. Typical pressure time history applied to the ANSYS model.

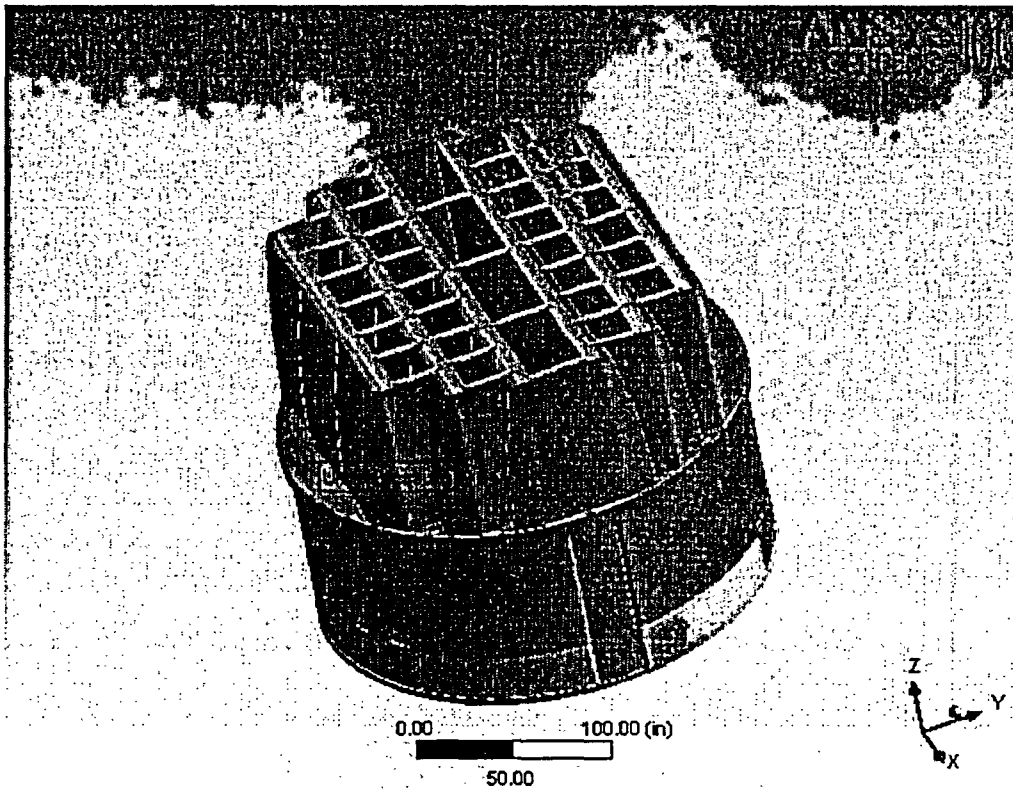


Figure 2.5. Surfaces with applied pressure loading.

III. Finite Element Model

The structure of the steam dryer was modeled using the ANSYS computer code.

3.1 Model Simplifications

Preliminary runs were made to determine areas of higher stress, so that model detail could be increased in these areas. The following simplifications were made in order to reduce model size and retain key structural properties:

- Most welds were replaced by geometrical constraints. In high stress locations welds were explicitly modeled by solid elements using a fine mesh.
- The drying vanes were replaced by point masses, placed onto the corresponding trough bottom plates (Figure 3.1). However, the bounding perforated plates, vane banks, and vane covers were explicitly modeled.
- The lower part of the skirt and drain channels were submerged in the reactor pool. An analysis was used to calculate the effective mass of this water, to account for its interaction with the structure. This added water mass was included in the ANSYS model.
- The steam dryer lifting rods were not modeled. Instead, they were replaced by fixed constraints at their connection to the trough bottom plates. Another fixed constraint was applied at the contact areas with the reactor vessel pins (Figure 3.2). All nodes in these locations were fixed.

3.2 Perforated Plate Model

The perforated plates were modeled as solid plates with adjusted elastic and dynamic properties. Properties of the perforated plates were assigned according to the type and size of perforation. Based on [2], the effective modulus of elasticity was found to be a factor of 0.6 times the original modulus, while the effective density was a factor of 0.8 times the original steel density. These adjusted properties were shown in Table 2.1.

3.3 Vane Bank Model

The vanes were modeled as point masses, located at the center of mass for each vane bank. The following masses were used for the vanes, based on data found on drawings supplied by PSE&G: inner banks, 6,500 lbm; middle banks, 5,900 lbm; and outer banks, 4,600 lbm. These weights were applied to the trough bottom plates.

3.4 Water Inertia Effect on Submerged Panels

Water inertia was modeled by an increase in density of the submerged structure. The added mass was found by an analysis to be 1.09 lbm/in^2 of submerged skirt area.

3.5 Structural Damping

Time history analysis in the ANSYS program requires that the damping be specified in terms of mass and stiffness Raleigh damping, i.e., α and β damping. These material constants can be defined from the damping ratio over the range of frequencies examined. For the calculation presented here, a damping ratio of 1% was assumed over the range of frequencies from 10 to 150 Hz. This assumption leads to the following values used in the analysis: $\alpha = 1.18$ and $\beta = 2 \times 10^{-5}$. This damping is consistent with guidance given in NUREG-1.61.

3.6. Mesh Details and Element Types

Shell elements were assumed for the skirt, drain channels, hoods, perforated plates, side and end panels, trough bottom plates, and cover plates. All other parts were modeled with solid elements, including tie bars, upper and lower support rings, vane covers, reinforcement plates, backing bars, and weld details.

Mesh details and element types are shown in Tables 3.1 and 3.2. Overall mesh design is shown in Figure 3.3. The mesh was refined at locations such as pipes / trough bottom plate junctions, tie bars and vane covers, welds, and the upper and bottom support ring. Typical examples are shown in Figures 3.4, 3.5, and 3.6.

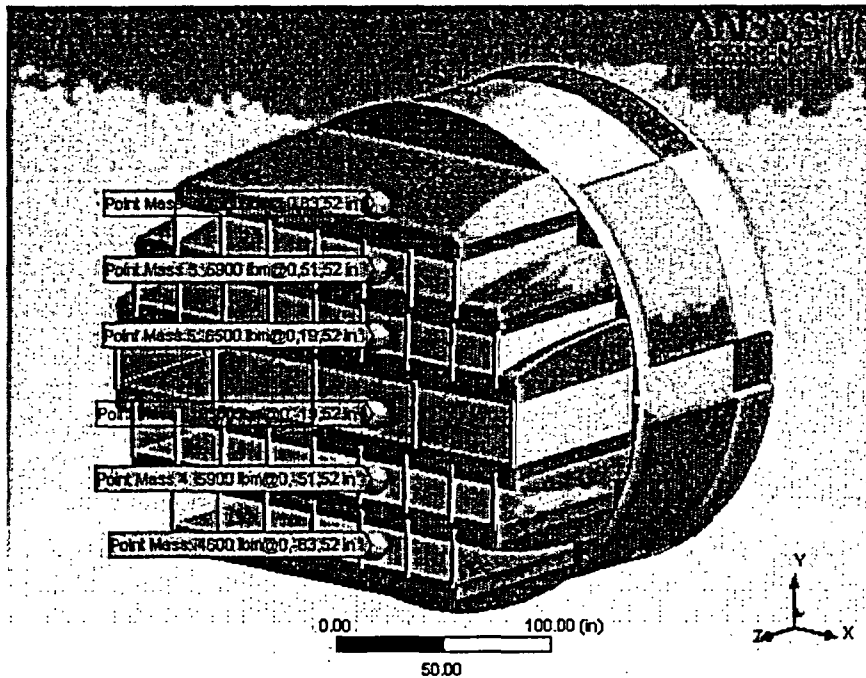


Figure 3.1. Point masses replaced the vanes.

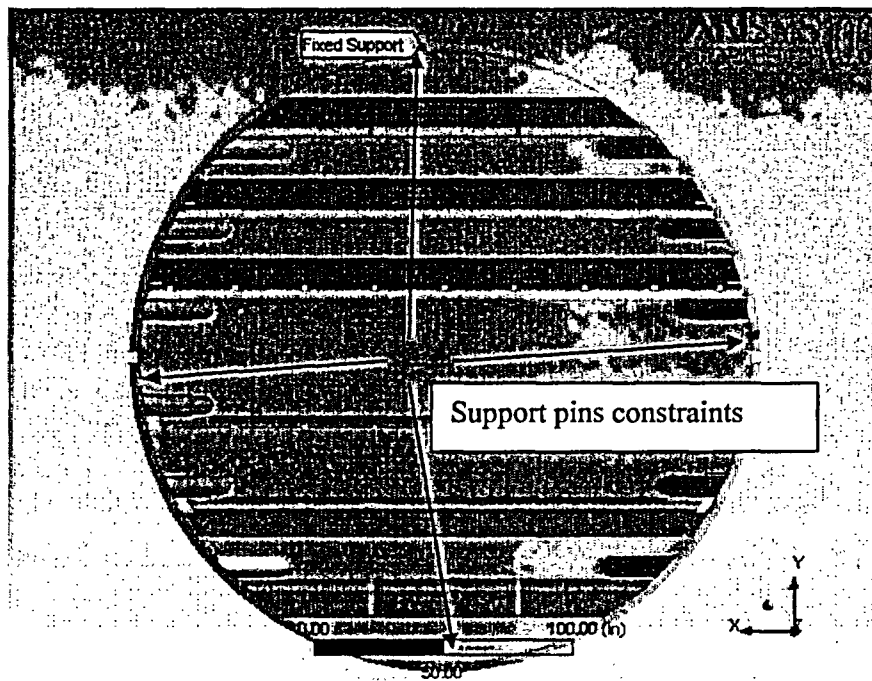
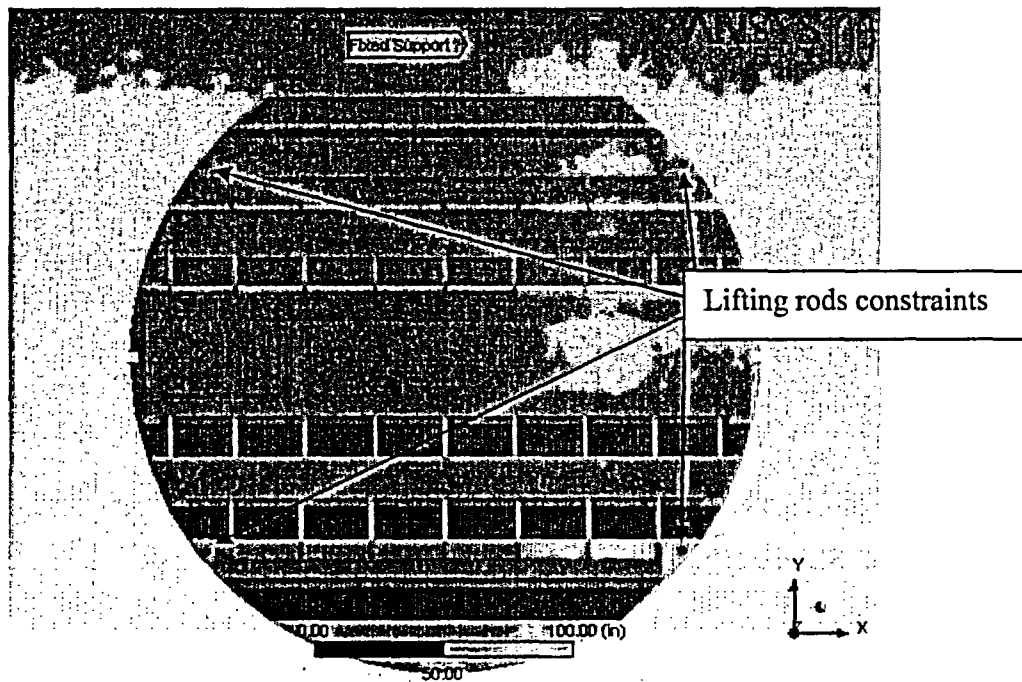


Figure 3.2. Fixed support constraints.

Table 3.1. Mesh Details

FE Model Summary	
Description	Quantity
Total Nodes	99,868
Total Elements	86,974
Total Body Elements	50,499
Total Contact Elements	36,475
Element Types	13
Materials	3
Thicknesses	113
Contacts	152

Table 3.2 Element Types.

Generic Element Type Name	NASTRAN Name	ANSYS Name
10-Node Quadratic Tetrahedron	Solid187	10-Node Tetrahedral Structural Solid
20-Node Quadratic Hexahedron	Solid186	20-Node Hexahedral Structural Solid
20-Node Quadratic Wedge	Solid186	20-Node Hexahedral Structural Solid
4-Node Linear Triangular Shell	Shell181	4-Node Structural Shell
4-Node Linear Quadrilateral Shell	Shell181	4-Node Structural Shell
Quadratic Quadrilateral Contact	Conta174	High-Order Surface to Surface Contact
Quadratic Quadrilateral Target	Targe170	Surface Contact Target
Quadratic Triangular Contact	Conta174	High-Order Surface to Surface Contact
Quadratic Triangular Target	Targe170	Surface Contact Target
Linear Quadrilateral Contact	Conta173	Low-Order Surface to Surface Contact
Linear Quadrilateral Target	Targe170	Surface Contact Target
Linear Triangular Contact	Conta173	Low-Order Surface to Surface Contact
Linear Triangular Target	Targe170	Surface Contact Target

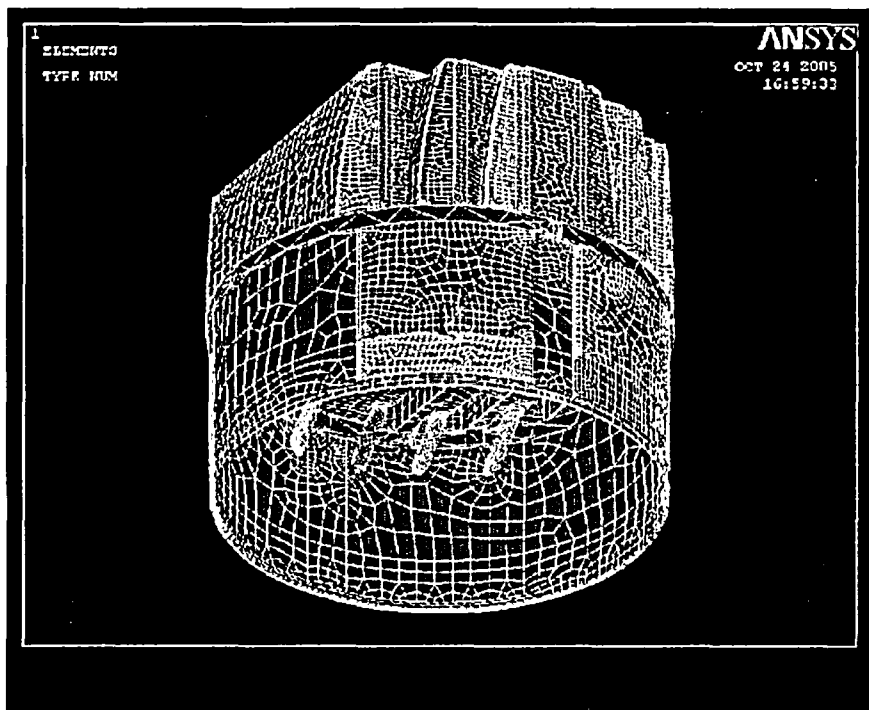
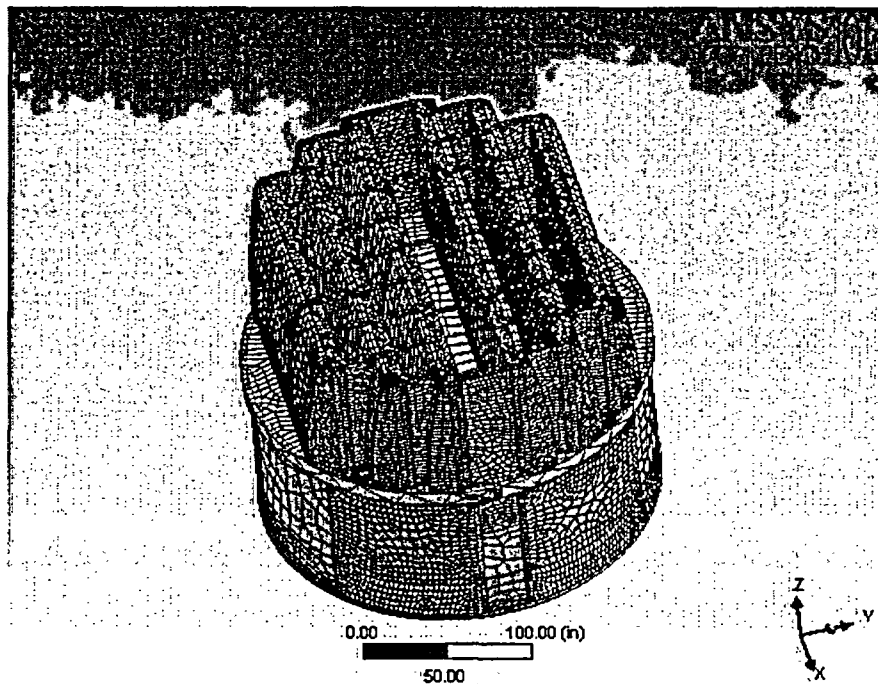


Figure 3.3. Mesh overview.

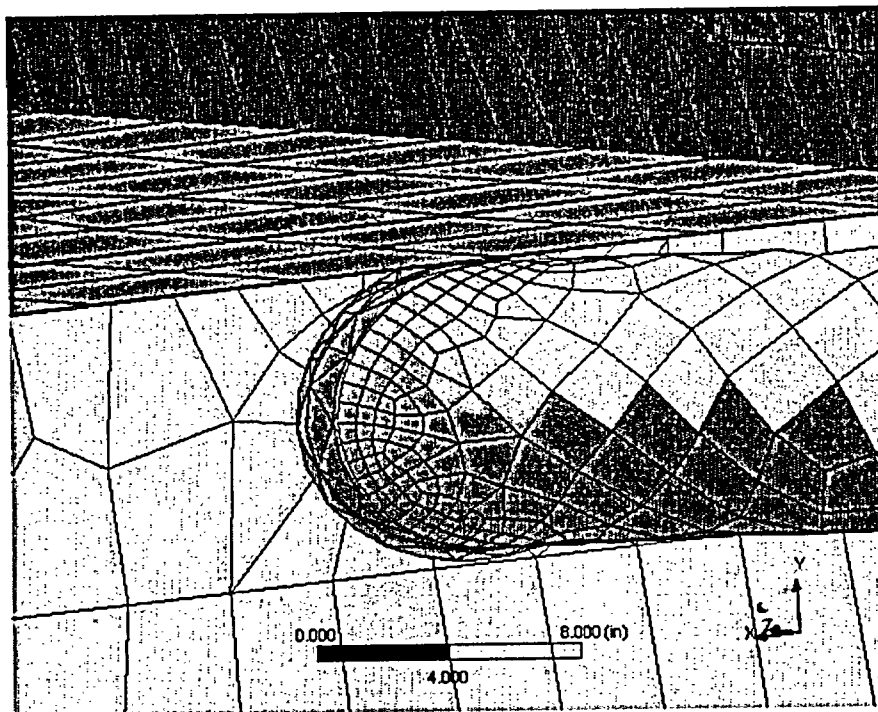


Figure 3.4. Mesh refinement example.

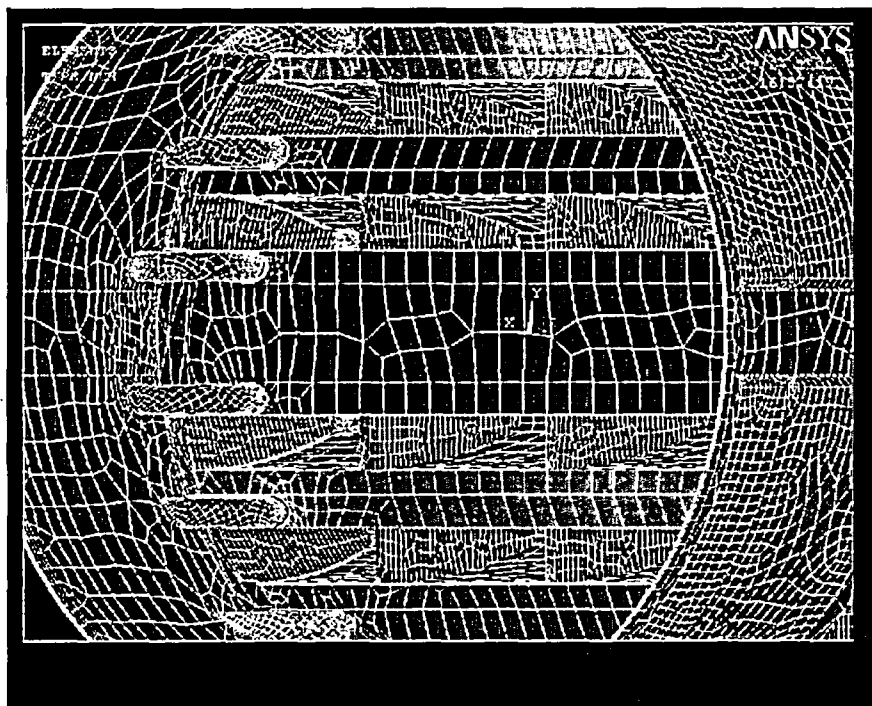
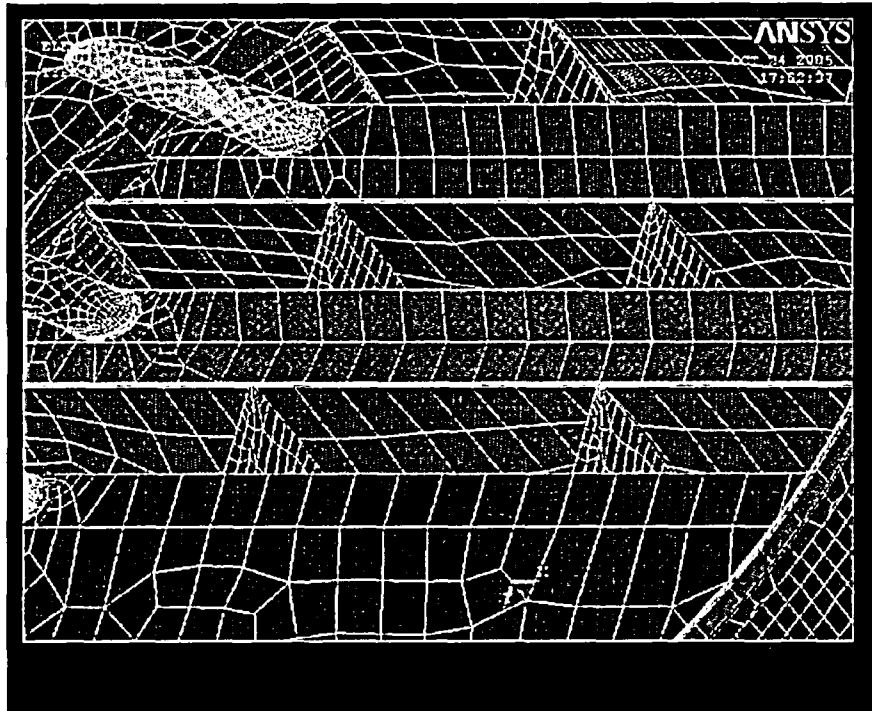


Figure 3.5. Mesh views from beneath the steam dryer.

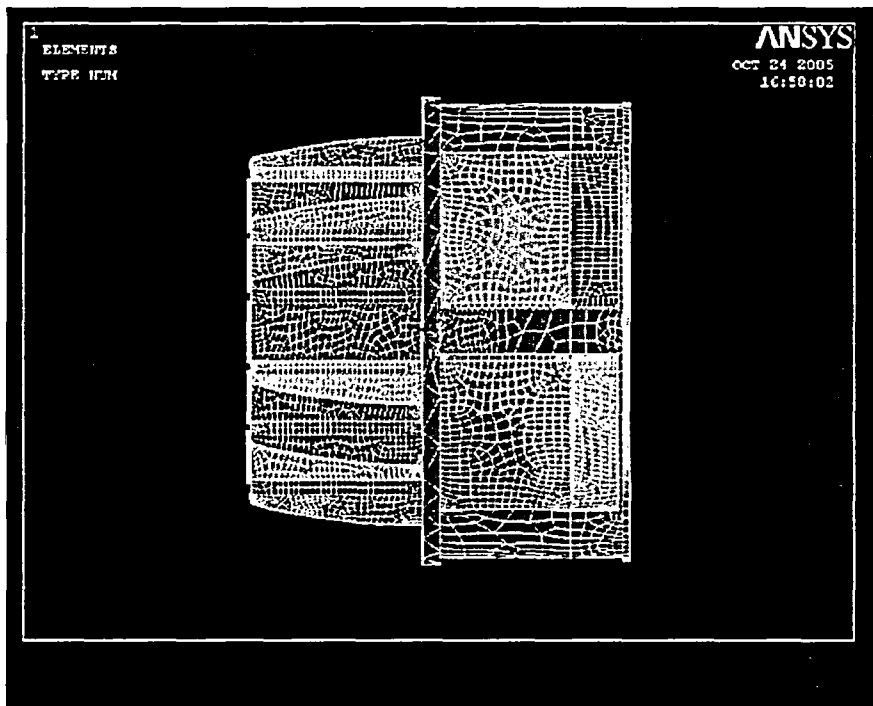
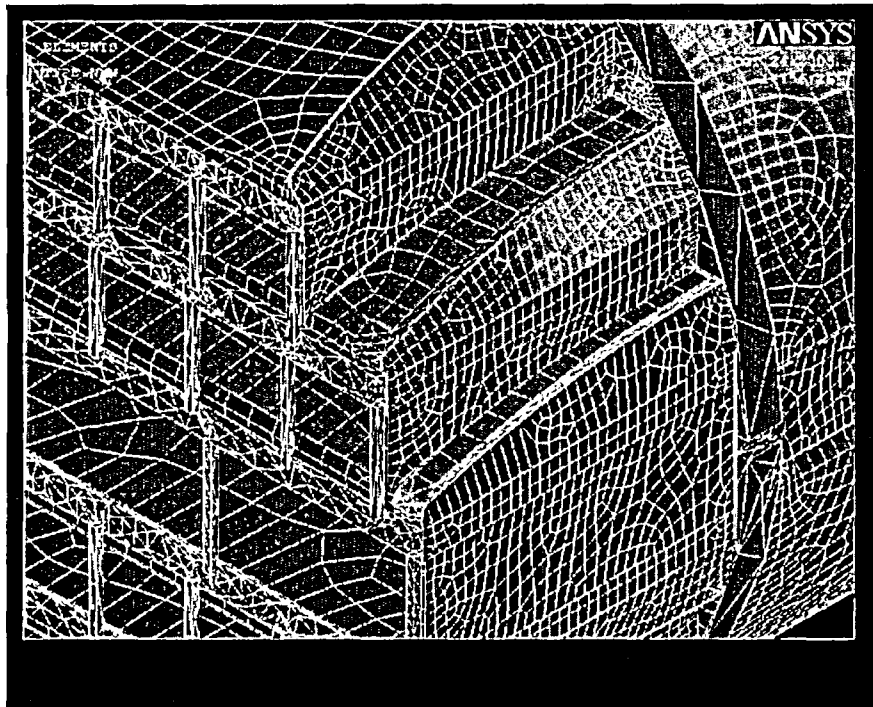


Figure 3.6. Mesh views of the sides of the steam dryer.

IV. Dynamic Analysis

The fluctuating pressure loads were applied to the structural model at all surface nodes described in Section 2.3. The pressures were varied at increments of 0.001 sec for 500 time steps – a total time of 0.5 sec. These stress results are discussed in Section V.

Stresses were calculated for each time increment, and a post-processor was used to determine the maximum stress times and to calculate the stress intensities at these time points. These stress intensities are then used in the evaluation in Section VI.

V. Results

5.1 General Stress Distribution

The ANSYS program provides contour plots of stress intensity based on smoothing of the nodal values over the surface. Typical contour plots, demonstrating stress intensity distribution over the structure, are shown in Figure 5.1. Note that stress intensities in most areas are very low (less than 500 psi); but there are areas with higher stress intensities, up to 3,000 to 4,000 psi.

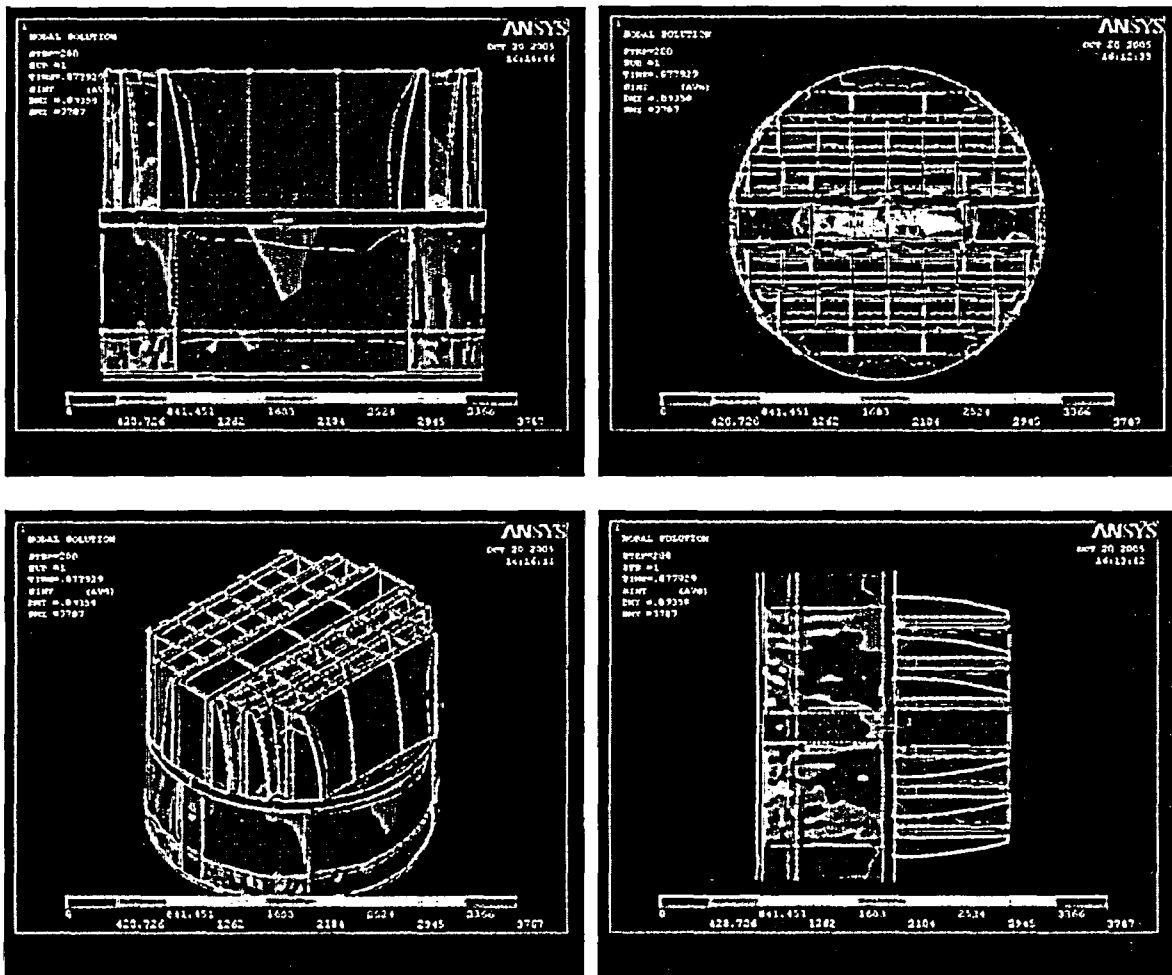


Figure 5.1. Stress intensity distribution at time step 200 of 500.

5.2 Maximum Stress Locations

Distribution of maximum stress intensity and maximum alternating stress intensity are shown in Figures 5.2 to 5.7. A stress summary is shown in Table 5.1. Values shown are read directly from the ANSYS output. Weld stresses must be adjusted for both maximum and alternating stress intensity as shown in Section VI.

Table 5.1. Locations with highest predicted stress intensities.

Location	Maximum Stress Intensity (psi)	Alternating Stress Intensity (psi)
Drain Channels	4,155	2,054
Weld / Drain Pipe / Trough Bottom Plates	3,648	675
Trough Bottom Plates Near Drain Pipes	3,216	696
Weld / Hood Support / Vane Banks	2,893	366
Weld / Side panel / Trough Bottom Plates	2,685	394
Inner Hood	2,450	1,270

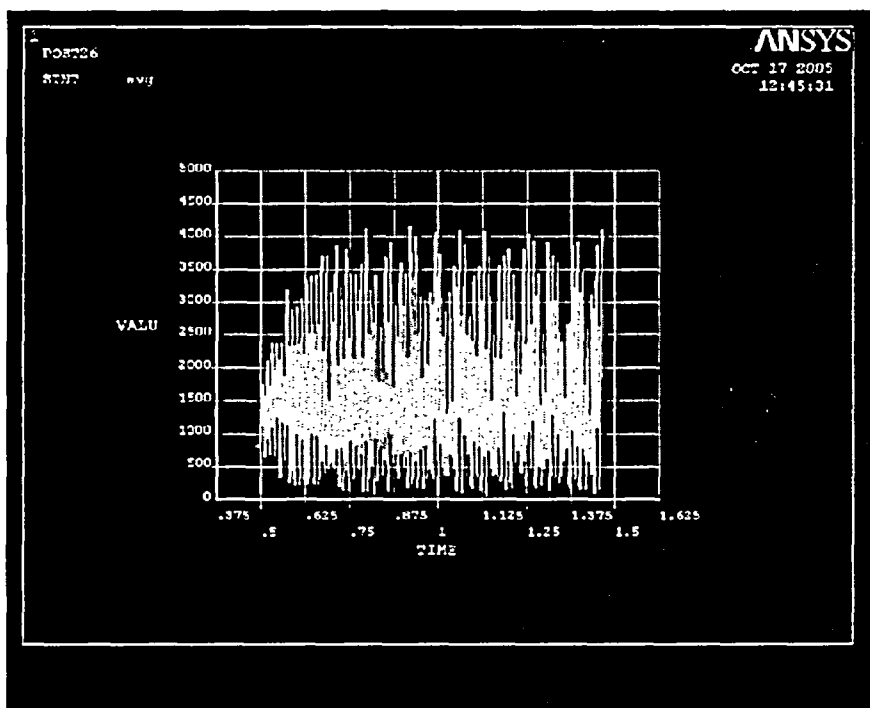
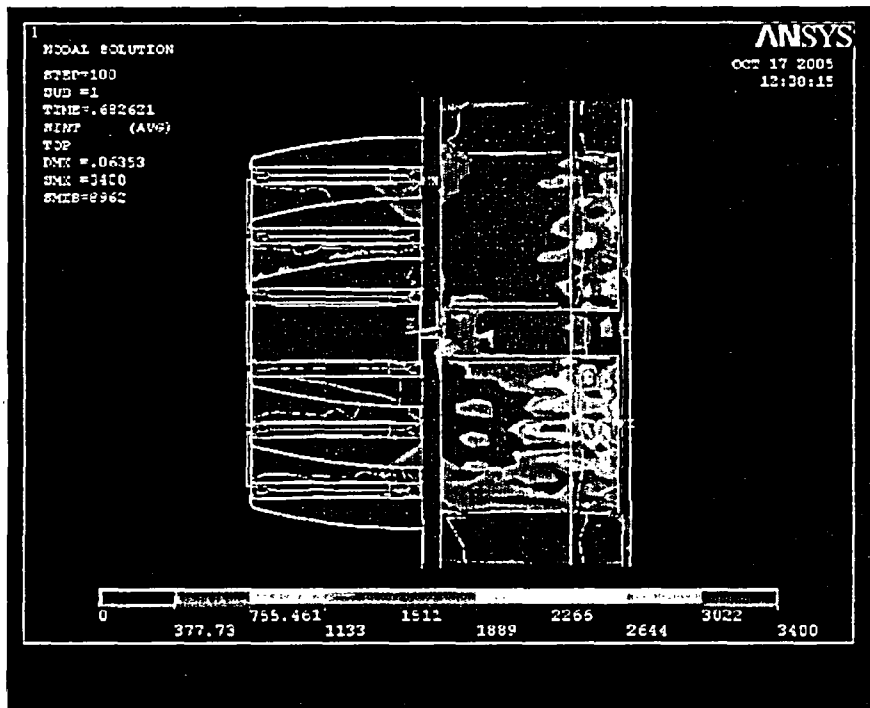


Figure 5.2. Maximum stress prediction occurs at the drain channels: stress contours (top); time history (bottom). The maximum stress intensity is 4,155 psi. The alternating stress intensity is 2,054 psi.

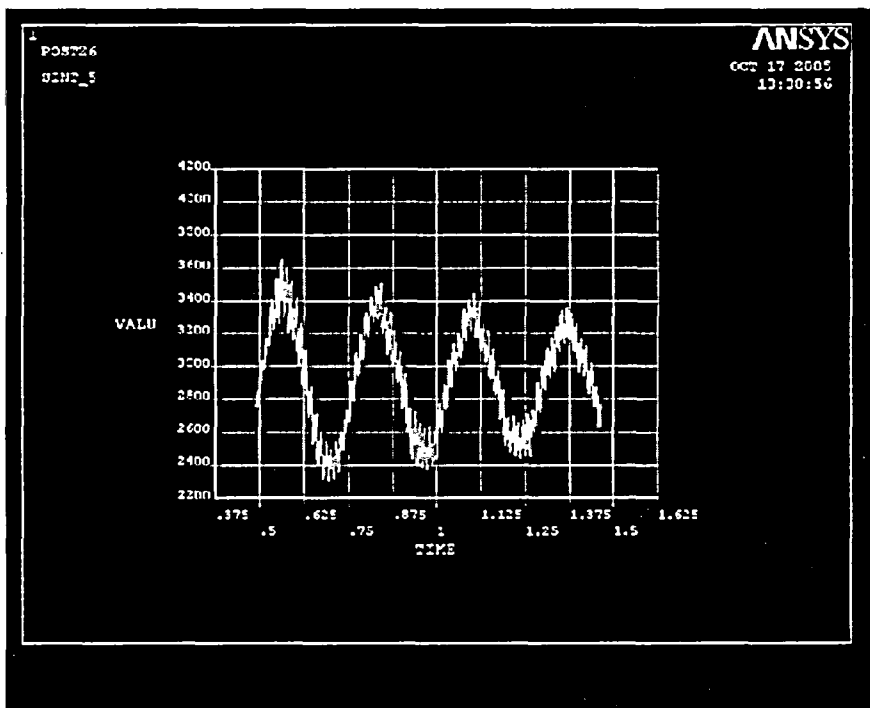
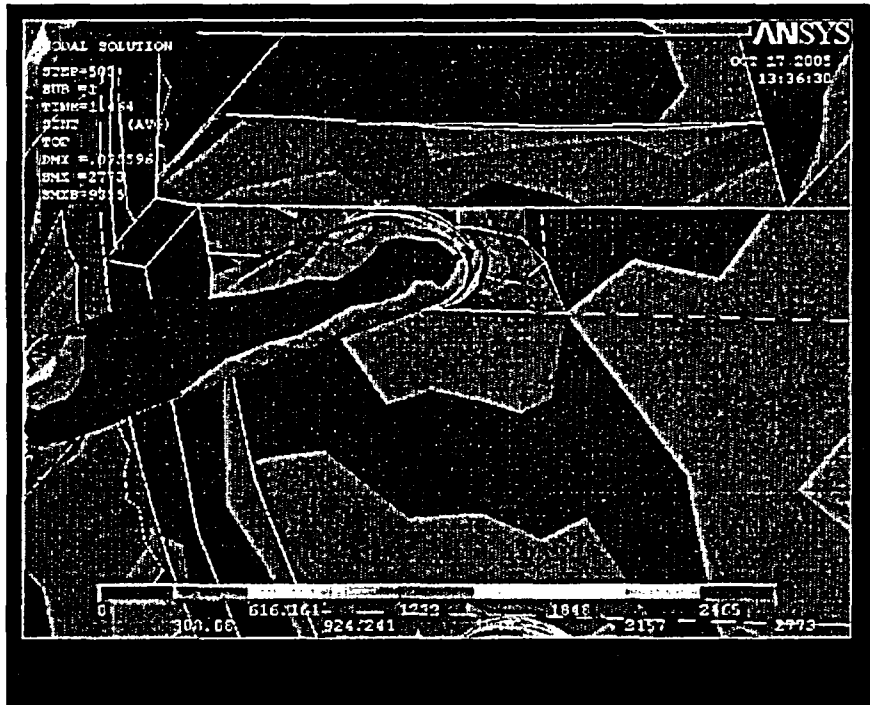


Figure 5.3. Stress prediction at the pipe / trough bottom plate welds: stress contours (top); time history (bottom). The maximum stress intensity is 3,648 psi. The alternating stress intensity is 675 psi.

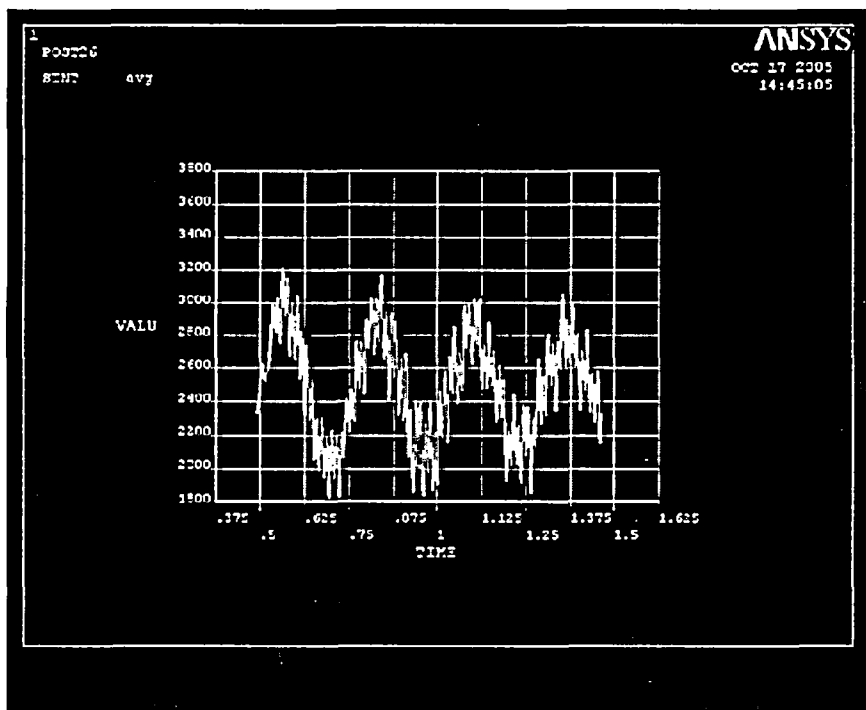


Figure 5.4. Stress prediction at the trough bottom location around welds: stress contours (top); time history (bottom). The maximum stress intensity is 3,216 psi. The alternating stress intensity is 696 psi.

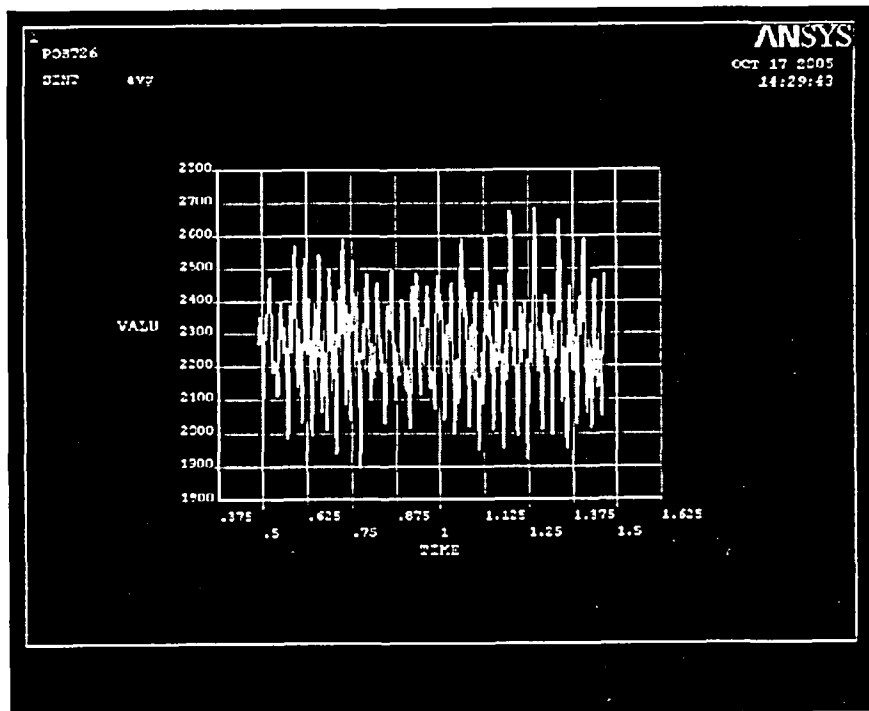
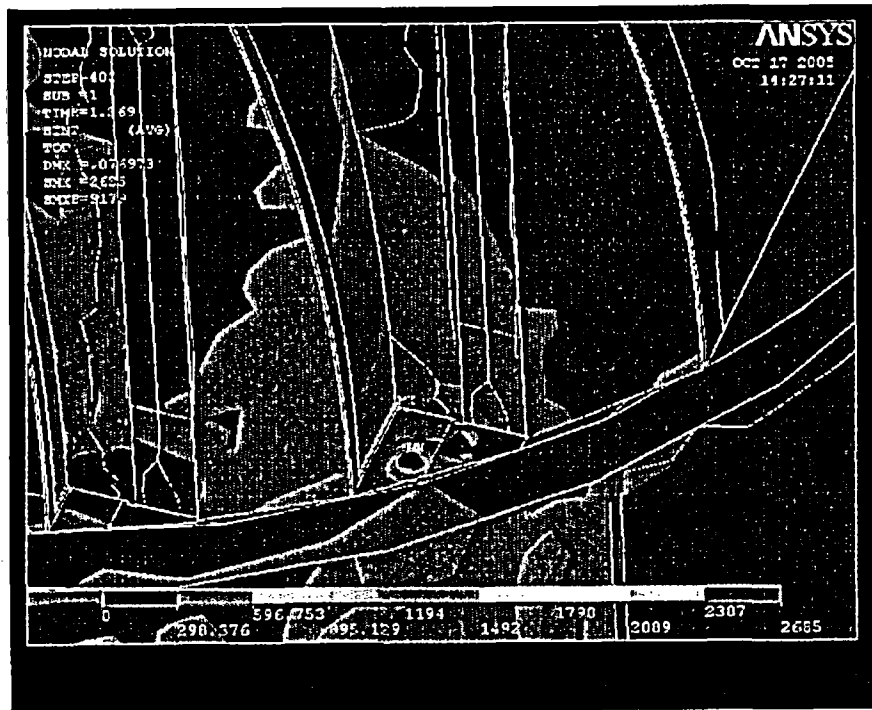


Figure 5.5. Stress prediction at the side panel welds to trough bottom plate / hood backing bar: stress contours (top); time history (bottom). The maximum stress intensity is 2,685 psi. The alternating stress intensity is 394 psi.

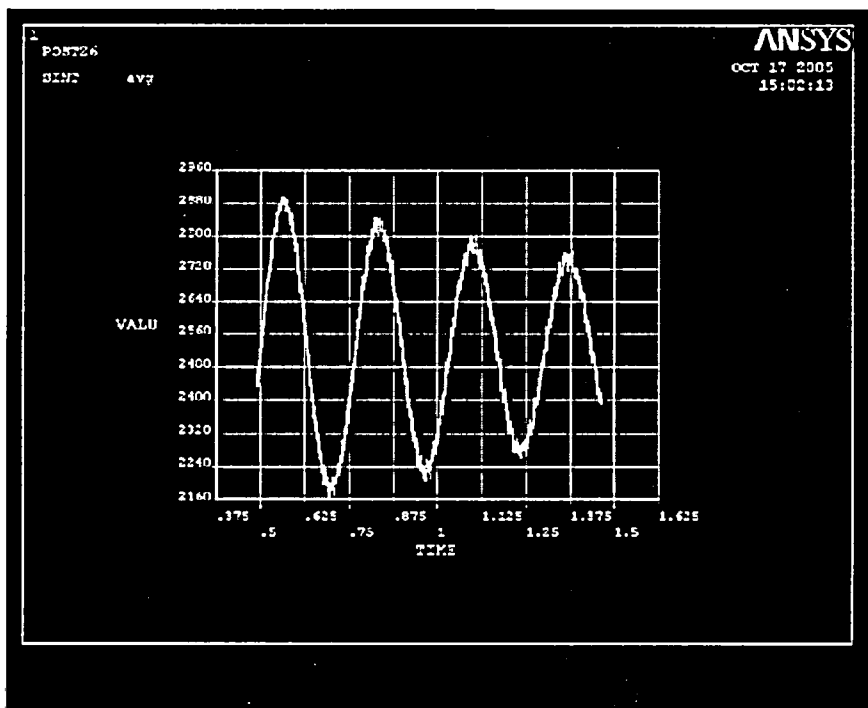
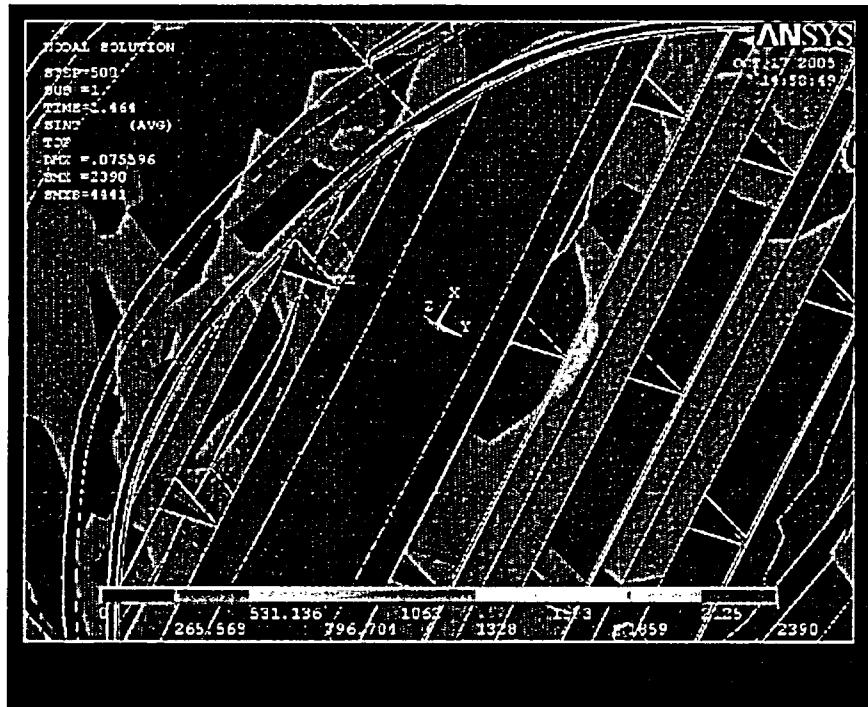


Figure 5.6. Stress prediction at the hood support and vane bank weld: stress contours (top); time history (bottom). The maximum stress intensity is 2,893 psi. The alternating stress intensity is 366 psi.

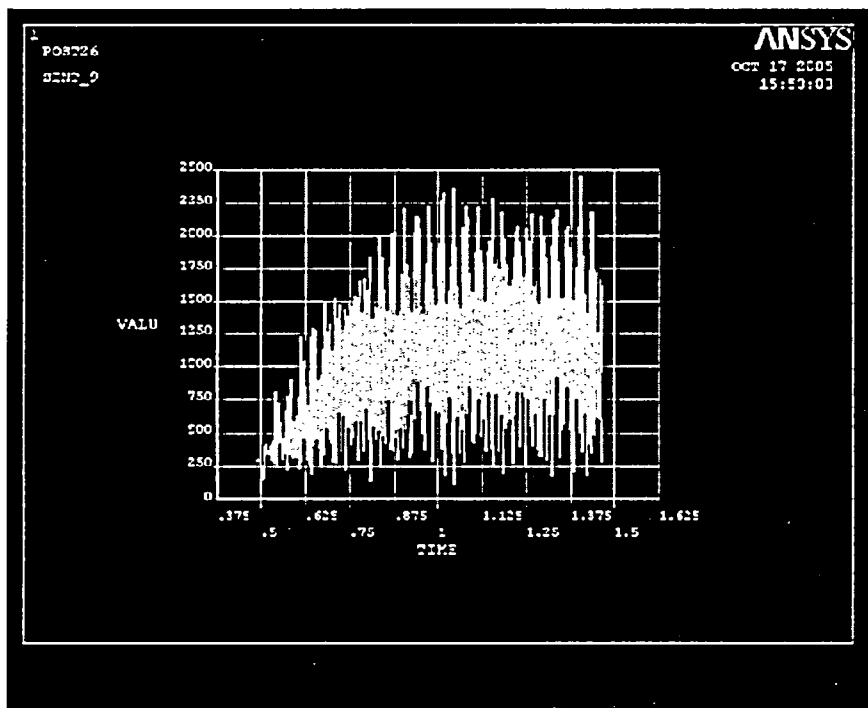
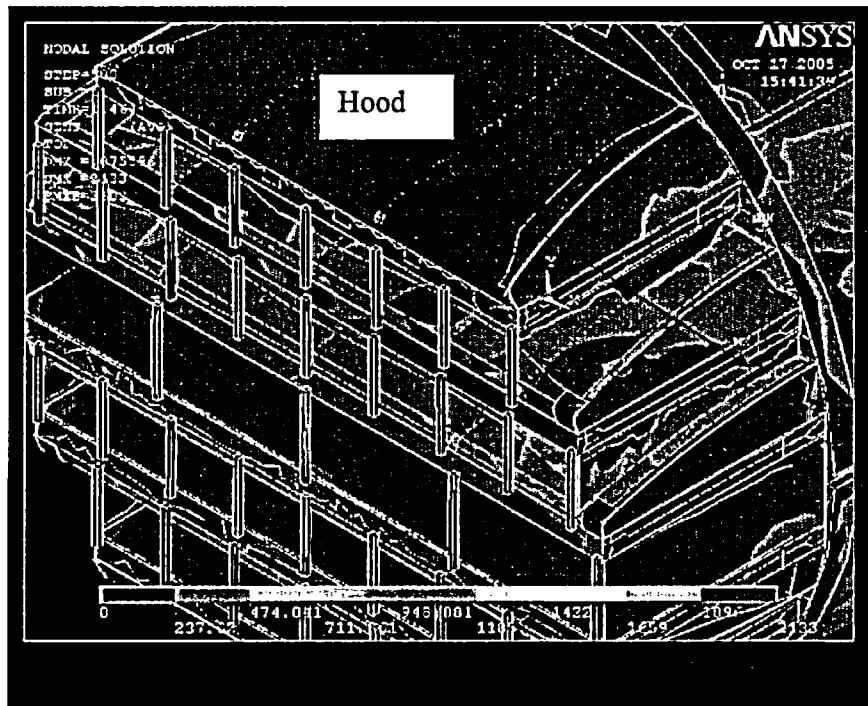


Figure 5.7. Stress prediction on an inner hood: stress contours (top); time history (bottom). The maximum stress intensity is 2,450 psi. The alternating stress intensity is 1,270 psi.

VI. Load Combinations and Allowable Stress Intensities.

6.1 Load Combinations for Evaluation

The ASME Code provides different allowable stresses for different load combinations and plant conditions. The stress levels of interest in this analysis are for the normal operating condition, which is the Level A service condition. The load combination for this condition is:

$$\text{Normal Operating Load Combination} = \text{Weight} + \text{Pressure} + \text{Thermal}$$

The weight and fluctuating pressure have been calculated in this analysis, and included in the stress results. The static pressure differences and thermal expansion stresses are small, since the entire steam dryer is suspended inside the reactor vessel and all surfaces are exposed to the same conditions. The large margins in the stress results easily accommodate any small contributions from these loads.

Seismic loads only occur in Level B and C cases, and are not considered in this analysis.

6.2 Allowable Stress Intensities

The ASME Code shows the following (Table 6.1) for the maximum allowable stress intensity (S_m) and alternating stress intensity (S_a) for the Level A service condition.

Table 6.1. Maximum Allowable Stress Intensity and Alternating Stress Intensity for all elements other than welds. The notation P_m represents membrane stress; P_b represents stress due to bending; Q represents secondary stresses (from thermal effects, for example); and F represents peak stresses (due to discontinuities, for example).

Type	Notation	Calculation	Allowable Value (psi)
General Membrane	P_m	S_m	18,300
Membrane + Bending	$P_m + P_b$	$1.5 S_m$	27,450
Primary + Secondary	$P_m + P_b + Q$	$3.0 S_m$	54,900
Primary + Secondary + Peak	$P_m + P_b + Q + F$	S_a	13,600

The limiting welds were modeled as solid elements to maximize the accuracy of the predicted values. In addition, when evaluating welds, either the calculated stress value was increased or the allowable stress value was decreased, as explained below, in order to include a stress concentration factor:

- For maximum allowable stress intensity, the allowable value is decreased by multiplying its value in Table 6.1 by 0.55.
- For alternating stress intensity, the calculated weld stress intensity is multiplied by a weld stress intensity (fatigue) factor of 1.8, before comparison to the S_a value given above.

The factors of 0.55 and 1.8 were selected based on the observable quality of the shop welds and NDE testing of all welds (excluding tack and intermittent welds) during fabrication. GE Purchase Specification for the HCGS Steam Dryer (21A9355 Section 9.2) called for liquid penetrant testing of all welds (excluding tack and intermittent welds) along the entire length or circumference, using the guidance of ASME Boiler and Pressure Code, Paragraph N-6127.3. In addition, critical welds are subject to periodical visual inspections in accordance with the requirements of GE SIL 644. Therefore, for weld stress intensities, the allowable values are shown in Table 6.2.

Table 6.2. Weld Stress Intensities.

Type	Notation	Calculation	Allowable Value (psi)
General Membrane	Pm	0.55 Sm	10,065
Membrane + Bending	Pm + Pb	0.825 Sm	15,098
Primary + Secondary	Pm + Pb + Q	1.65 Sm	30,195
Primary + Secondary + Peak	Pm + Pb + Q + F	Sa	13,600

6.3 Comparison of Calculated and Alternating Stress Intensities

Areas with the highest stress intensities are listed below, in Table 6.3, along with the allowable stresses.

Table 6.3. Comparison of Calculated and Allowable Stress Intensities. Stress ratio is the ratio of allowable stress intensity to calculated stress intensity.

Location	Type of Stress	Calculated Stress Intensity (psi)	Allowable Stress Intensity (psi)	Stress Ratio
Drain Channels (Lower Portion)	Pm + Pb	4,155	27,450	6.6
	Sa	2,054	13,600	6.6
Weld / Drain Pipe to Trough Bottom Plate	Pm + Pb	3,648	15,098	4.1
	Sa	1,215	13,600	11.2
Trough Bottom Plate (Area Near Drain Pipe Weld)	Pm + Pb	3,216	27,450	8.5
	Sa	696	13,600	19.5
Weld / Outer Hood Interior Vertical Hood Support Plate to Vane Bank	Pm + Pb	2,893	15,098	5.2
	Sa	659	13,600	20.6
Weld / Outer Hood Outlet Plenum End Plate to Bottom of Trough	Pm	2,685	10,065	3.7
	Sa	709	13,600	19.2
Inner Hood, Curved Plate	Pm	2,450	18,300	7.5
	Sa	1,270	13,600	10.7

VII. Conclusions

The dynamic analysis of the steam dryer at Hope Creek Unit 1 shows that the steam flow and gravity loads produce stresses that meet all of the allowable stress values of the ASME, B&PV Code, Section III, subsection NG. Since these loads represent practically the full load condition for normal operation (Level A Service Level), we conclude that the steam dryer will continue to operate without structural failure.

Maximum points of stress and the calculated / allowable stress ratios are tabulated in Section VI of this report. This tabulation shows a minimum stress ratio of 3.7. Almost all other locations on the steam dryer have significantly lower stresses than those listed in Section VI.

VII. References

1. Continuum Dynamics, Inc. 2005. Hydrodynamic Loads on Hope Creek Unit 1 Steam Dryer to 200 Hz. C.D.I. Report No. 05-17.
2. Meijers, P. 1895. Refined Theory for Bending and Torsion of Perforated Plates. *Journal of Pressure Vessel Technology* 108: 423-429.